BIOCHIP JOURNAL, Vol. 3, No. 3, 237-248, September 2009

Proteomic Profiling of Human Hepatocellular Carcinoma Tissues by Two-Dimensional Electrophoresis and Mass Spectrometry

Seok Joo Hong[1,†], Jongmin Kim[1,†], Jun Ho Park[1], Eun Kyung Lim[1], Jinpyo Kim[1], Yoon Jung Choi[2], HongDu Gu[3], Seung Whan Kim[4], Kwan Yong Choi[5], Jae-Won Joh[6] & Dae Shick Kim[7]

[1]CbsBioscience, Inc., 59-5 Jang-Dong, Yuseong-gu, Daejeon 305-343, Korea
[2]Department of Pathology, National Health Insurance Corporation Ilsan Hospital, Goyang-city, Gyeonggi-do 410-719, Korea
[3]Department of Emergency Medicine, National Health Insurance Corporation Ilsan Hospital, Goyang-city, Gyeonggi-do 410-719, Korea
[4]Department of Emergency Medicine, Chungnam National University Hospital, Daejeon 301-721, Korea
[5]Department of Life Science, Pohang University of Science and Technology, Pohang 790-784, Korea
[6]Department of Surgery, Samsung Medical Center, Sungkyunkwan University School of Medicine, Seoul 135-710, Korea
[7]Department of Pathology, Samsung Medical Center, Sungkyunkwan University School of Medicine, Seoul 135-710, Korea
[†]These authors contributed equally to this work
Correspondence and requests for materials should be addressed to K.Y. Choi (kchoi@postech.ac.kr) and D.S. Kim (oncorkim@skku.edu)

Accepted 18 July 2009

Abstract

Hepatocellular carcinoma (HCC) is the most common tumor in the adult liver, with high relapse and mortality rates despite diverse treatment modalities. To identify novel HCC markers, we analyzed HCC and paired nontumor tissues from five early HCC patients (Edmondson grade I and II) by two-dimensional gel electrophoresis (2-DE) and matrix-assisted laser desorption/ionization time-of-flight (MALDI-TOF) mass spectrometry (MS). To obtain a detailed proteome map, narrow pH-range strips were utilized in the isoelectric focusing (IEF) step. A total of 44 2-D gels were obtained and more than 1,000 protein spots were detected. We successfully identified 85 differentially expressed protein spots, including 49 up-regulated and 36 down-regulated spots in HCC tissues, corresponding to 74 different proteins (44 up-regulated and 30 down-regulated). These differentially expressed proteins included well-known deregulated proteins in HCC such as heat shock protein (HSP) family and proliferating cell nuclear antigen (PCNA), consistent with previous studies. All 74 proteins were classified according to their functional categories described by Gene Ontology, shedding light on processes deregulated in hepatocarcinogenesis. Thirty-three proteins have not been reported in other HCC proteomic profiling analysis and, in particular, overexpression of transketolase (TKT) and second mitochondria-derived activator of caspase/direct inhibitor of apoptosis-binding protein with low pI (Smac/DIABLO) could be novel candidate markers for HCC. In summary, we profiled proteome alterations in HCC tissues, and these results may provide useful diagnostic and prognostic markers of HCC.

Keywords: Hepatocellular carcinoma, Proteomics, Biomarker, 2DE, MALDI-TOF MS

Introduction

Hepatocellular carcinoma (HCC) is the fifth most common cancer worldwide and the most common form of liver cancer, being responsible for 80% of primary malignant tumors in adults. HCC causes more than 600,000 deaths annually worldwide and its endemic prevalence in Asia and Africa makes HCC one of the top causes of death in this region[1]. It is known that HCC develops from chronic inflammatory liver disease due to the hepatitis B virus (HBV) infection, hepatitis C virus (HCV) infection, and exposure to carcinogens such as aflatoxin B1[2]. Liver cancer is often asymptomatic at the early and most curable stages; hence, patients are usually diagnosed at very advanced stages upon presentation when effective treatments are unavailable. The current standard diagnosis of HCC relies on the detection of the serum alpha-fetoprotein (AFP) level in at-risk subjects. This is followed by hepatic ultrasonography and computed tomography to identify suspicious nodules. The serum AFP level has limited use as a diagnostic marker due to its low sensitivity (41-65%), whereas the diagnostic imaging method is highly operator-dependent with high false-negative rates particularly when the tumor nodule is <2 cm in diameter[3]. Today, there is no effective biomarker for the early detection of HCC or for monitor-

Table 1. Characteristics of the patients involved in this study.

Patient No.	Age	Gender	HBV	HCV	AFP (ng/mL)	Edmondson grade	Tumor size (cm)
1	66	Male	−	+	690.5	I	2.7*2.5*1.5
2	53	Male	+	−	−	I	3.7*3.5*2.8
3	65	Male	+	−	28	II	8.8*8.7*6.9
4	58	Male	+	−	6.3	II	5.2*4.7*4.3
5	62	Male	+	−	8798.1	II	5*5.1*4.4

ing its recurrence[4,5]. Therefore, identifying early detection markers of HCC is vital for afflicted patients in order for them to receive therapeutic benefits from curative surgery.

Over the past decade, the proteomic approach has proved useful as a key technology in the global analysis of protein expression related to malignancies such as cancer[6]. Two-dimensional polyacrylamide gel electrophoresis (2-DE) and matrix-assisted laser desorption/ionization time-of-flight (MALDI-TOF) mass spectrometry (MS) are among the most common and powerful tools in proteomics approaches. Proteomic analysis including 2-DE and MALDI-TOF-MS was recently applied to tissue samples from patients with HCC, leading to the identification of several protein targets differentially expressed in HCC[7-12]. Such approaches are expected to yield novel diagnostic and prognostic biomarkers and therapeutic targets for human cancers in the postgenomic era. However, the reported candidate markers are only partially coincident due to the differences in sampling and proteomics techniques[7-15]. Moreover, few of these candidate markers are undergoing clinical development and evaluation in larger patient populations[16]. Therefore, further development of candidate biomarkers would necessarily require a focused analysis on the proteome of early tumor tissues in a relatively homogeneous patient cohort.

In the present work, a comprehensive and comparative analysis is made of the proteins associated with HCC using 2-DE and MALDI-TOF MS to identify the proteins related to hepatocarcinogenesis. We identified 74 differentially expressed proteins between five sets of HCC tissues (Edmondson grade I and II) and adjacent paired nontumorous tissues. These differentially expressed proteins were statistically analyzed and classified into Gene Ontology categories. Thirty-three proteins have not been reported in other HCC proteomic profiling analysis and, in particular, the overexpression of transketolase (TKT) and second mitochondria-derived activator of caspase/direct inhibitor of apoptosis-binding protein with low pI (Smac/DIABLO) could be novel candidate markers for HCC. These results provide a foundation for the search for potential diagnostic and prognostic markers and therapeutic targets for HCC.

Results

Differential Proteome Expression between HCC and Surrounding Nontumorous Tissues

Five sets of HCC and nontumorous surrounding tissues obtained from male HCC patients with similar pathological characteristics were used. All five cases were in Edmondson grade I or II with an average age of 60.8 years (53-66). Pathologic data of the five cases are shown in Table 1. In order to examine the differential proteome expression to investigate important tumor-interrelated proteins, the proteomes of five pairs of clinical HCC tissue samples were separated by high-resolution 2-DE. To obtain a detailed proteome map, four types of 18 cm immobilized pH gradient (IPG) gel strips were used in the first dimension: pI 3-11 nonlinear, pI 3-5.6 nonlinear, pI 5.3-6.5 linear, and pI 6.2-7.5 linear. Up to 500 μg of total protein samples were successfully separated with narrow pI-range IPG strips (pI 3-5.6 nonlinear, pI 5.3-6.5 linear, and pI 6.2-7.5 linear), allowing for a better enrichment of important HCC-related proteins. The second dimension separation was through 12% SDS polyacrylamide gels. For one patient (case #1), two frozen samples from different sections of a single tumor were analyzed to test the variability of tumor specimen and the reproducibility of 2-DE. A total of 44 2-D gels were obtained, and the most reproducible gels from each sample were selected for statistical analysis. More than 1,000 protein spots were detected on the 2-D gels, and the images were analyzed using Progenesis Samespots software. The proteome profiles of HCC tumor tissue and adjacent paired nontumorous tissue (case #3) are shown in Figure 1.

Detection and Identification of Differentially Expressed Proteins

Based on Progenesis Samespots software analysis, the ratios of normalized spot volumes of tumor to paired nontumor tissue were calculated, and spots showing more than a 1.5-fold difference on average were selected. MALDI-TOF MS was first used to analyze the peptides after in-gel digestion. The ten most intense peptide ions for each spot were selected and further

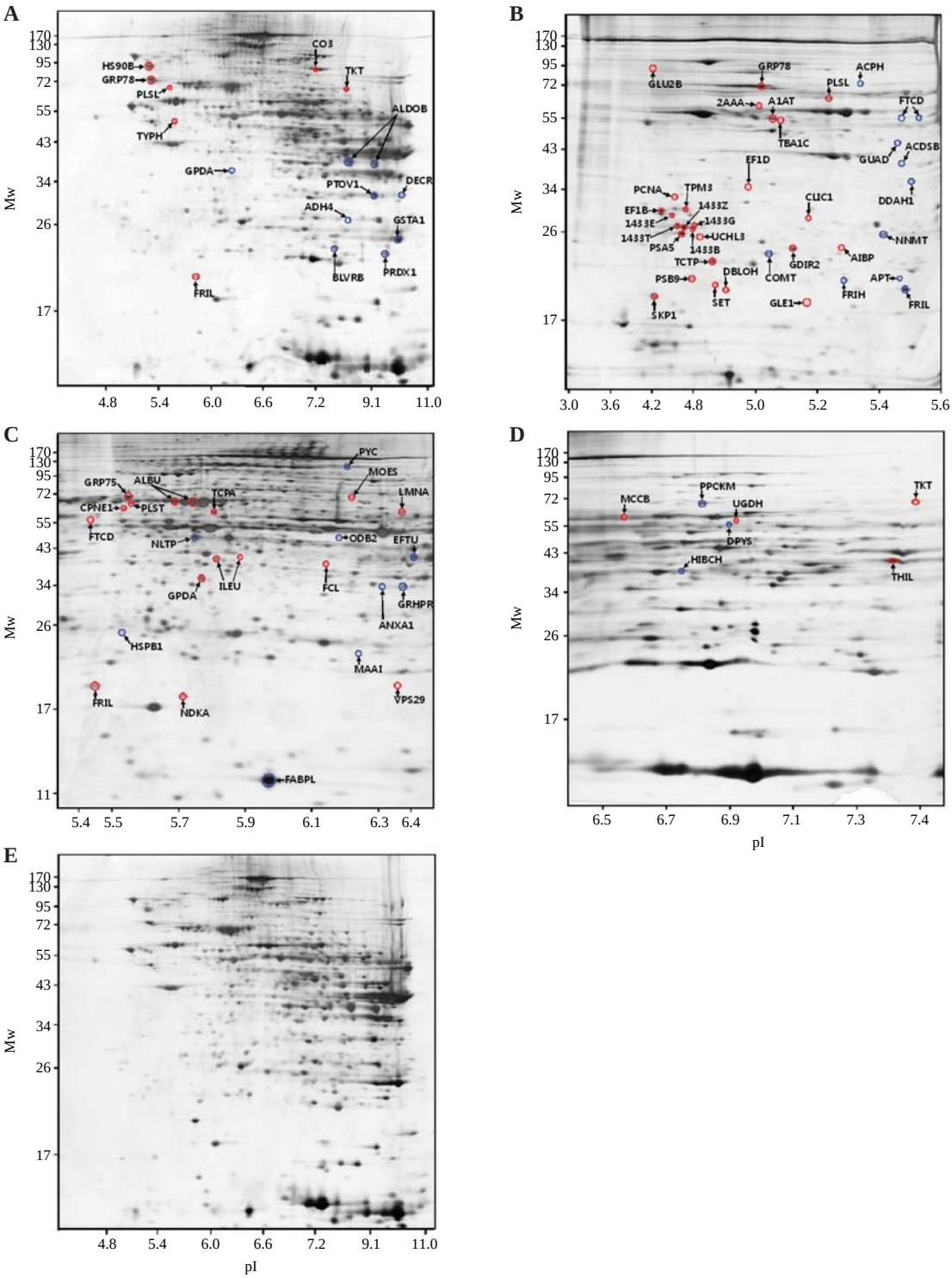

Figure 1. 2-DE patterns of whole-cell proteins obtained from (A-D) HCC tissue and (E) adjacent paired nontumorous tissue (case #3). Silver-stained 2-D gels with narrow-range IPG strips for nontumorous tissue are not shown. The pI ranges and total protein loads for 2-D gels are as follows: (A) pI 3-11 nonlinear, 100 µg HCC proteins, (B) pI 3-5.6 nonlinear, 500 µg HCC proteins, (C) pI 5.3-6.5 linear, 500 µg HCC proteins, (D) pI 6.2-7.5 linear, 500 µg HCC proteins, (E) pI 3-11 nonlinear, and 100 µg nontumorous tissue proteins. The protein spots identified in this study are circled and labeled with Uniprot IDs. Forty-nine spots corresponding to 44 proteins showed higher levels in HCC tissues compared to nontumorous surrounding tissues (red circles), while 36 spots corresponding to 30 proteins showed lower levels in HCC tissues compared to nontumorous surrounding tissues (blue circles).

Table 2. In total, 74 proteins with differential expression (≥1.5-fold increase or decrease) between HCC and paired nontumor tissue were identified by MALDI-TOF MS and MS/MS.

UniProt ID	Fold change	UniProt description	Ref	Theoretical Mw/pI	Identification method	Molecular function	Cellular component	Biological process
LMNA	5.0±6.7	Lamin-A/C	Y	65.1/6.40	PMF	binding	cell part	
SET	4.5±3.1	Protein SET	N	28.8/5.76	MS/MS	binding	cell part	metabolic process
PSB9	4.0±3.2	Proteasome subunit beta type-9 precursor (EC 3.4.25.1)	N	22.3/4.92	MS/MS	catalytic activity	cell part	immune system process
TCTP	3.4±2.4	Translationally-controlled tumor protein	Y	19.6/4.84	MS/MS	binding	organelle	cellular process
TKT	3.0±2.0	Transketolase (EC 2.2.1.1)	N	67.8/7.90	MS/MS	binding	cell part	metabolic process
1433T	2.6±1.8	14-3-3 protein theta	N	27.7/4.68	MS/MS	binding	organelle	biological regulation
GLU2B	2.5±1.9	Glucosidase 2 subunit beta precursor	N	59.3/4.34	MS/MS	binding	organelle	cellular process
GLE1	2.5±1.2	Nucleoporin GLE1	N	75.4/6.58	PMF	binding	cell part	cellular process
PCNA	2.5±0.6	Proliferating cell nuclear antigen	Y	28.8/4.57	MS/MS	binding	membrane-enclosed lumen	metabolic process
DBLOH	2.4±1.2	Diablo homolog	N	20.7/4.80	PMF	binding	cell part	cellular process
PLSL	2.4±1.0	Plastin-2	N	70.2/5.20	MS/MS	binding	cell part	
1433G	2.3±0.8	14-3-3 protein gamma	Y	28.2/4.80	MS/MS	binding	cell part	cellular process
1433Z	2.3±0.9	14-3-3 protein zeta/delta	N	27.7/4.73	MS/MS	binding	organelle	cellular process
CLIC1	2.2±1.2	Chloride intracellular channel protein 1	Y	26.9/5.09	MS/MS	binding	cell part	cellular process
1433B	2.2±0.8	14-3-3 protein beta/alpha	N	28.1/4.76	MS/MS	binding	cell part	cellular process
EF1B	2.1±1.1	Elongation factor 1-beta	N	24.7/4.50	MS/MS	binding	cell part	metabolic process
VPS29	2.1±1.2	Vacuolar protein sorting-associated protein 29	N	20.5/6.29	MS/MS	binding	organelle	localization
GRP78	2.1±0.5	78 kDa glucose-regulated protein precursor	Y	72.3/5.07	MS/MS	binding	cell part	cellular process
GDIR2	2.1±1.2	Rho GDP-dissociation inhibitor 2	Y	23.0/5.10	MS/MS	enzyme regulator activity	organelle	immune system process
TPM3	2.1±1.0	Tropomyosin alpha-3 chain	Y	29.0/4.75	MS/MS	binding	organelle	cellular process
ILEU	2.0±0.7	Leukocyte elastase inhibitor	Y	42.7/5.90	PMF	enzyme regulator activity	cell part	
MOES	2.0±0.7	Moesin	N	67.8/6.08	MS/MS	binding	cell part	immune system process
HS90B	1.9±0.7	Heat shock protein HSP 90-beta	Y	83.2/4.97	MS/MS	binding	organelle	metabolic process
SKP1	1.9±0.8	S-phase kinase-associated protein 1	N	18.6/4.40	MS/MS	binding	cell part	metabolic process
TYPH	1.9±0.9	Thymidine phosphorylase precursor (EC 2.4.2.4)	N	49.9/5.36	MS/MS	binding	cell part	metabolic process

Table 2. Continued.

UniProt ID	Fold change	UniProt description	Ref	Theoretical Mw/pI	Identification method	Molecular function	Cellular component	Biological process
FCL	1.8±1.0	GDP-L-fucose synthetase (EC 1.1.1.271)	N	35.9/6.12	MS/MS	binding	cell part	metabolic process
AIBP	1.7±1.1	Apolipoprotein A-I-binding protein precursor	N	26.1/5.27	MS/MS	binding	extracellular region	
UCHL3	1.7±0.9	Ubiquitin carboxyl-terminal hydrolase isozyme L3	Y	26.2/4.84	MS/MS	catalytic activity	cell part	metabolic process
UGDH	1.7±0.6	UDP-glucose 6-dehydrogenase (EC 1.1.1.22)	Y	55.0/6.73	MS/MS	binding		metabolic process
PSA5	1.7±0.8	Proteasome subunit alpha type-5 (EC 3.4.25.1)	N	26.4/4.74	MS/MS	binding	cell part	metabolic process
MCCB	1.7±0.4	Methylcrotonoyl-CoA carboxylase beta chain	N	61.3/7.57	MS/MS	catalytic activity	membrane-enclosed lumen	metabolic process
PLST	1.6±0.5	Plastin-3	N	70.8/5.41	MS/MS	binding		
NDKA	1.6±0.9	Nucleoside diphosphate kinase A (EC 2.7.4.6)	Y	20.4/7.07	MS/MS	binding	cell part	metabolic process
TBA1C	1.6±0.4	Tubulin alpha-1C chain	N	49.9/4.96	PMF	binding	organelle	cellular process
A1AT	1.6±0.5	Alpha-1-antitrypsin precursor	Y	46.7/5.43	MS/MS	binding	membrane-enclosed lumen	multicellular organismal process
EF1D	1.6±0.6	Elongation factor 1-delta	Y	31.1/4.90	PMF	binding	cell part	metabolic process
THIL	1.6±0.6	Acetyl-CoA acetyltransferase	Y	45.3/9.07	MS/MS	binding	membrane-enclosed lumen	metabolic process
1433E	1.5±0.7	14-3-3 protein epsilon	N	29.2/4.63	MS/MS	binding	organelle	cellular process
TCPA	1.5±0.3	T-complex protein 1 subunit alpha	Y	60.3/5.80	MS/MS	binding	cell part	metabolic process
2AAA	1.5±0.5	PP2A, subunit A, PR65-alpha isoform	N	64.4/5.10	PMF	binding	cell part	metabolic process
GRP75	1.5±0.3	Heat shock 70 kDa protein 9	Y	73.6/5.87	MS/MS	binding	cell part	metabolic process
CO3	1.5±0.3	Complement C3 precursor	Y	71.1/6.82	PMF	binding	extracellular region part	immune system process
ALBU	1.5±0.4	Serum albumin precursor	Y	69.0/5.85	MS/MS	binding	membrane-enclosed lumen	cell killing
CPNE1	1.5±0.4	Copine-1	N	59.1/5.52	PMF	binding		metabolic process
BLVRB	−1.5±0.4	Flavin reductase (EC 1.5.1.30)	Y	22.1/7.13	MS/MS	binding	cell part	metabolic process
PYC	−1.5±0.7	Pyruvate carboxylase	N	129.5/6.47	MS/MS	binding	membrane-enclosed lumen	metabolic process
NLTP	−1.5±0.5	Non-specific lipid-transfer protein (EC 2.3.1.176)	Y	59.0/6.44	PMF	binding	organelle	metabolic process
ACPH	−1.6±0.5	Acylamino-acid-releasing enzyme (EC 3.4.19.1)	Y	81.2/5.29	MS/MS	electron carrier activity	cell part	metabolic process
EFTU	−1.6±0.6	Elongation factor Tu	Y	49.5/7.70	PMF	binding	membrane-enclosed lumen	metabolic process

Table 2. Continued.

UniProt ID	Fold change	UniProt description	Ref	Theoretical Mw/pI	Identification method	Molecular function	Cellular component	Biological process
HSPB1	−1.6±0.3	Heat shock 27 kDa protein	Y	22.8/5.98	MS/MS	binding	cell part	cellular process
PTOV1	−1.6±0.6	Prostate tumor overexpressed gene 1 protein	N	31.5/9.84	PMF		cell part	biological regulation
ANXA1	−1.6±0.6	Annexin A1	Y	35.0/7.77	MS/MS	binding	cell part	metabolic process
PRDX1	−1.7±0.4	Peroxiredoxin-1 (EC 1.11.1.15)	Y	20.7/6.41	MS/MS	binding	organelle	metabolic process
GRHPR	−1.7±0.6	Glyoxylate reductase/ hydroxypyruvate reductase	N	26.9/6.90	PMF	binding	cell part	metabolic process
HIBCH	−1.7±0.5	3-hydroxyisobutyryl-CoA hydrolase	N	42.9/8.34	MS/MS	binding	organelle	metabolic process
ODB2	−1.9±0.7	Dihydrolipoamide branched chain transacylase	N	53.5/8.71	PMF	binding	membrane-enclosed lumen	metabolic process
FRIL	−2.0±0.9	Ferritin light chain	Y	20.0/5.51	MS/MS	binding	macromolecular complex	cellular process
GSTA1	−2.1±1.0	Glutathione S-transferase A1 (EC 2.5.1.18)	Y	25.6/8.84	MS/MS	catalytic activity	cell part	metabolic process
PPCKM	−2.1±1.0	Phosphoenolpyruvate carboxykinase	Y	70.5/7.21	MS/MS	binding	organelle	metabolic process
ACDSB	−2.2±1.2	Short/branched chain specific acyl-CoA dehydrogenase	Y	47.5/6.53	PMF	binding	membrane-enclosed lumen	metabolic process
DPYS	−2.2±1.3	Dihydropyrimidinase (EC 3.5.2.2)	N	56.6/6.81	MS/MS	binding	cell part	metabolic process
DDAH1	−2.2±1.5	N(G),N(G)-dimethylarginine dimethylaminohydrolase 1	Y	31.1/5.53	MS/MS	binding	cell part	metabolic process
GPDA	−2.3±1.1	Glycerol-3-phosphate dehydrogenase	Y	37.5/5.81	PMF	binding	cell part	metabolic process
ADH4	−2.3±0.8	Alcohol dehydrogenase 4 (EC 1.1.1.1)	Y	40.2/8.25	MS/MS	binding	cell part	metabolic process
GUAD	−2.3±1.3	Guanine deaminase (EC 3.5.4.3)	Y	51.0/5.44	PMF	binding	cell part	metabolic process
DECR	−2.3±1.4	2,4-dienoyl-CoA reductase	Y	36.0/9.35	MS/MS	binding	organelle	metabolic process
FRIH	−2.4±1.2	Ferritin heavy chain (EC 1.16.3.1)	N	21.2/5.12	MS/MS	binding	macromolecular complex	immune system process
FTCD	−2.5±1.6	Formimidoyltransferase-cyclodeaminase	Y	58.9/5.58	PMF	binding	organelle	metabolic process
COMT	−2.6±2.0	Catechol O-methyltransferase (EC 2.1.1.6)	Y	24.4/5.15	MS/MS	binding	cell part	metabolic process
ALDOB	−2.6±1.8	Fructose-bisphosphate aldolase B (EC 4.1.2.13)	Y	39.5/7.98	MS/MS	binding	organelle	metabolic process
MAAI	−3.1±2.2	Maleylacetoacetate isomerase (EC 5.2.1.2)	N	24.1/7.60	MS/MS	binding	cell part	metabolic process
APT	−3.1±2.0	Adenine phosphoribosyltransferase	N	19.6/5.78	MS/MS	binding	cell part	metabolic process
NNMT	−3.2±2.8	Nicotinamide N-methyltransferase (EC 2.1.1.1)	Y	29.6/5.56	PMF	catalytic activity	cell part	
FABPL	−3.6±2.0	Fatty acid-binding protein, liver	Y	14.2/6.60	MS/MS	binding	cell part	multicellular organismal process

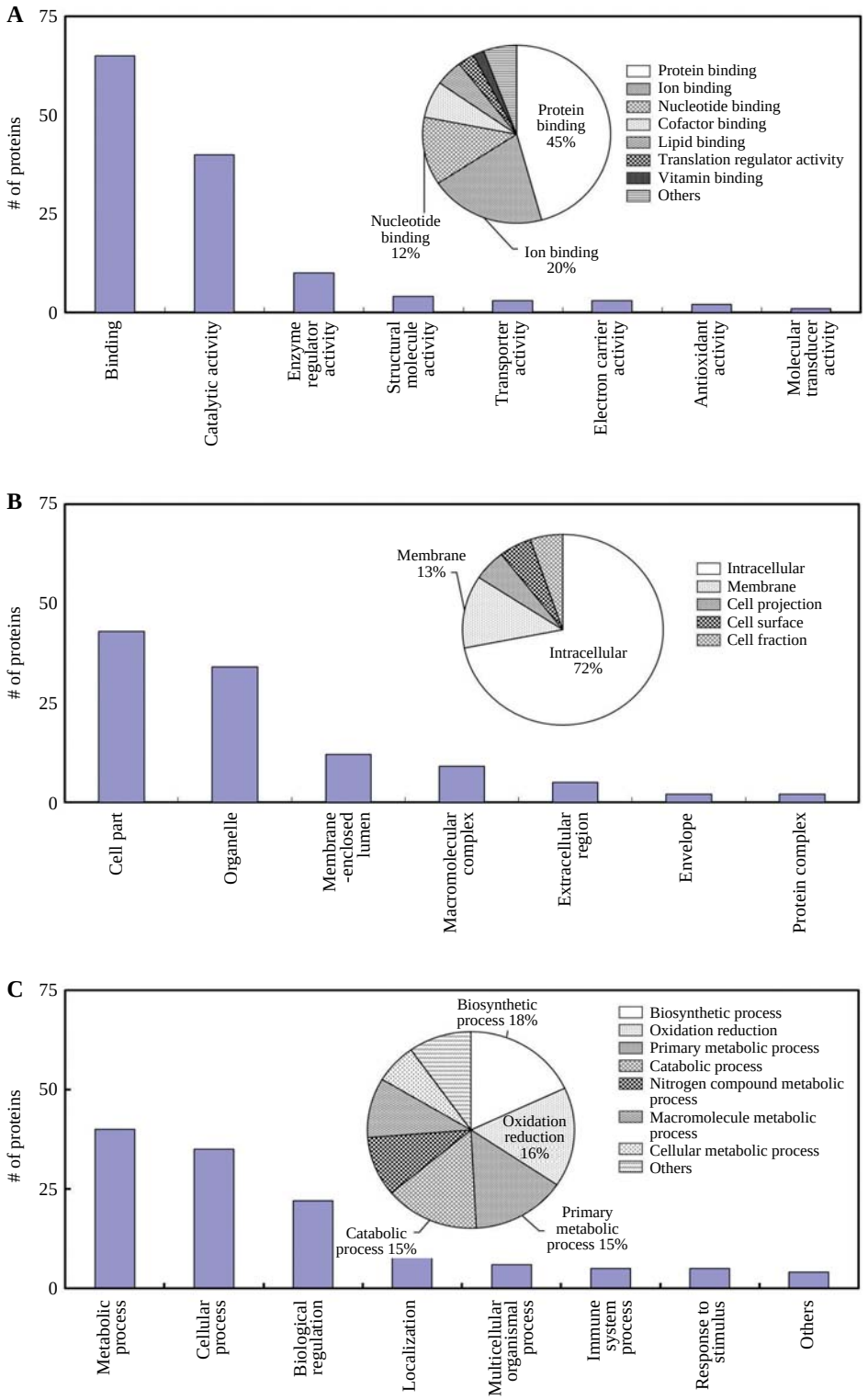

Figure 2. Gene Ontology classification of the 74 differentially expressed proteins identified by MALDI-TOF MS and MS/MS. (A) The 74 proteins were classified by molecular function terms. Binding was the largest class comprising 65 proteins (88%), followed by catalytic activity comprising 40 proteins (54%). (B) The 74 proteins were classified by cellular component terms. Cell part was the largest class comprising 43 proteins (58%). (C) The 74 proteins were classified by biological process terms. Metabolic process was the largest class comprising 40 proteins (54%). The smaller pie-charts in (A), (B), and (C) show the sub-classes of major categories. Several multifunctional proteins have been sorted into more than one subclass.

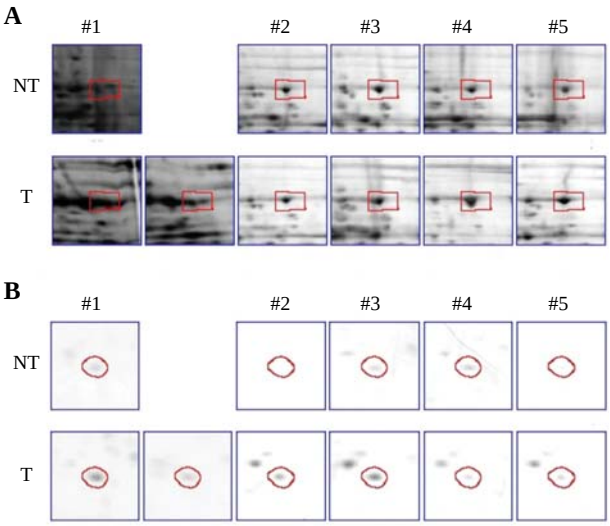

Figure 3. 2-DE spot images of (A) TKT and (B) Smac/DIABLO with increased expression levels in HCC tissues. (A) All HCC tissues showed up-regulation of TKT with fold-changes of more than 1.5 except for case #2. (B) All HCC tissues showed up-regulation of Smac/DIABLO with fold-changes of more than 1.5 except for case #4.

analyzed by MALDI-TOF MS/MS. A total of 85 protein spots, including 49 up-regulated and 36 down-regulated spots in HCC tissues corresponding to 74 different proteins were finally identified (Figure 1 and Table 2).

All 74 differentially expressed proteins were classified by their Gene Ontology terms. Figure 2 shows the proportions of each subclass listed in Table 2. In brief, binding was the largest class in molecular function terms, comprising 65 proteins (88%), followed by catalytic activity, which comprised 40 proteins (54%). Protein binding was the most common term, followed by ion binding and nucleotide binding among the binding subclass (Figure 2A). Cell part was the largest class in cellular component terms, comprising 43 proteins (58%), of which intracellular proteins were dominant followed by membrane proteins (Figure 2B). Metabolic process was the largest class in biological process terms, comprising 40 proteins (54%). Biosynthesis, oxidation/reduction, primary metabolic, catabolic and nitrogen compound metabolic processes were all enriched terms in metabolic processes (Figure 2C).

Among the 74 differentially expressed proteins, 41 proteins have been reported in previous proteomics research. The most significantly up-regulated protein in our proteomic data, Lamin A/C, has been reported[16,17]. Other up-regulated proteins included heat shock protein (HSP) family, 78 kDa glucose-regulated protein and HSP 90 beta, and proliferating cell nuclear antigen (PCNA), consistent with previous reports[10,12,16]. Similarly, some of the most significantly down-regulated proteins, such as fatty acid-binding protein (FABPL), nicotinamide N-methyltransferase (NNMT), and fructose-bisphosphate aldolase B (ALDOB) have been reported[12,14,18,19].

Taken together, the results show that the present proteome analysis is consistent with previous studies. Furthermore, 33 novel potential biomarker candidates associated with HCC were identified. Two novel up-regulated proteins, TKT and Smac/DIABLO, are of special interest due to their functional importance and reliable identification in all HCC specimens analyzed[20-23]. The 2-DE maps of TKT and Smac/DIABLO spots are shown in Figure 3A and B, respectively. TKT was identified by the MASCOT database search using the MS/MS raw data of peptides, which showed a significant match of two tryptic peptide fragments for TKT (7% coverage). Smac/DIABLO was identified by a MASCOT database search using the MS raw data of peptides, which showed a significant match of nine tryptic peptides for Smac/DIABLO (45% coverage).

Discussion

Over the past decade, there has been a surge of disease proteomics research, especially in the area of cancer proteomics. Several proteomic studies have analyzed HCC cell lines[24-26] and animal models of HCC[27,28], as well as human HCC samples[7-12]. Human serum is a type of clinical sample that is readily accessible by researchers. Thus, much attention has been paid to comparisons of sera among populations with different stages of chronic liver disease and HCC[29-31], and new research techniques such as the detection of glycosylated proteins have been applied[32]. However, the high-abundance proteins in human sera interfere with the detection of potential disease markers; therefore, overcoming a wide dynamic range remains a challenge for serum and plasma proteome analyses. Naturally, even if secreted, the disease-related proteins in serum or plasma would be significantly diluted compared to the tissue origins, where those proteins are highly concentrated. Therefore, a focused study of HCC tissues could offer a better starting point for biomarker discovery processes.

We analyzed the proteome of paired tumor and non-tumor liver tissues from five HCC patients using 2-DE and MALDI-TOF MS and MS/MS techniques. To obtain a high-resolution proteome map, four types of IPG gel strips were used in the isoelectric focusing step, leading to a successful identification of 74 differentially expressed proteins. It was found that the differ-

entially expressed proteins were consistent with other proteome profiles[10,12,14,16,18,19]. Moreover, 33 novel potential biomarker candidates associated with HCC were identified in this study.

Multistep pathogenesis of HCC involves complicated genetic and epigenetic changes[33-36]. As such, a better appreciation of the perturbations in multiple signaling pathways is greatly needed. In our proteomic data, hepatic metabolism, including the metabolism of substances and energy metabolism showed the most distinct changes between HCC and nontumor tissues. Gene Ontology term analysis of differentially expressed proteins identified 40 proteins (54%) related to metabolic processes. One of the key metabolic enzymes found in this study and previous studies is NNMT[14,18]. NNMT catalyzes the N-methylation of nicotinamide, pyrimidines, and other structural analogues, playing an important role in biotransformation and drug metabolism[37,38]. A recent report on the NNMT mRNA level as a prognostic marker of HCC indicates that the proteomic approach could identify valuable markers with potential clinical application[39]. Among the 33 newly identified biomarker candidates, two novel up-regulated proteins, TKT and Smac/ DIABLO, are of special interest due to their functional importance and reliable identification in all HCC specimens analyzed[20-23]. Interestingly, TKT mRNA overexpression has been reported as a poor prognostic factor in a large-scale RT-PCR analysis of HCC tissues[40]. Therefore, TKT protein merits further investigation as potential diagnostic and prognostic biomarker with a larger cohort of HCC patients.

Conclusions

We performed 2-DE combined with MS to analyze the proteomic profiling of HCC and their surrounding nontumorous tissues obtained from five HCC patients. We identified the discriminative and informative protein spots associated with Edmondson grade I and II HCCs. We confirmed that the proposed method is able to identify known HCC-related proteins such as HSP family, PCNA, and NNMT[10,12,14,16,18]. This confirms that our proteome analysis is consistent with many prior studies. Moreover, by using narrow-range IPG strips for a detailed proteome analysis, we were able to identify 33 novel potential biomarker candidates associated with HCC. Two overexpressed proteins, TKT and Smac/DIABLO, are particularly of interest because of their functional importance in the pentose phosphate pathway and apoptosis, respectively[20-23]. Recently, we found that TKT mRNA overexpression is correlated with poor prognosis in HCC patients[40]; therefore, it is likely that the TKT protein expression level is also useful as a prognostic marker in HCC. Although this study involved only a small number of samples, our proteomic strategy can be applied for the detection of diagnostic and prognostic biomarkers and for validation with a large number of HCC specimens.

Materials and Methods

Patients and Tissue Samples

HCC and corresponding non-cancerous hepatic tissues were obtained with informed consent from five patients who underwent curative hepatectomy for primary HCC in the Department of Surgery, Samsung Medical Center, Korea. The study protocol was approved by the Institutional Review Board of Samsung Medical Center. Complete clinical data were available in all five cases. The patients, ranging in age from 53 to 66 years (mean, 60.8 years) and having adequate liver function reserve, had survived for at least two months after hepatectomy, and none received treatment prior to surgery such as transarterial chemoembolization or radiofrequency ablation. The clinicopathologic features of the five HCCs in this study are described in Table 1. Surgically resected specimens were partly embedded in paraffin after fixation in 10% formalin for histological processing and partly immediately frozen in liquid nitrogen and stored at −80°C. Tumor grading was based on the criteria proposed by Edmondson and Steiner (I, well differentiated; II, moderately differentiated; III, poorly differentiated; IV, undifferentiated)[41]. HCC samples from two patients were classified as Edmondson grade I and HCC samples from three patients were classified as Edmondson grade II.

Sample Preparation

Human liver tissues were dissolved at a concentration of approximately 50 mg/mL in lysis buffer (50 mM Tris, 100 mM KCl, 20% Glycerol, pH 7.1) containing protease inhibitors. After grinding in a liquid nitrogen-cooled mortar and pestle, the samples were sonicated on ice for 2 min using an ultrasonic processor (BANDELIN) and centrifuged at 50,000 rpm for 1 hr at 4°C to remove DNA, RNA and any particulate materials. We collected the supernatant of samples and then extracted total proteins with 10% TCA precipitation (soluble fraction). The concentrations were measured by a modified Bradford assay (Bio-Rad). All samples were stored at −80°C until use.

2-DE and Image Analysis

The first dimension of IPG-DALT 2-DE was carried

out using multiphor II IEF system (Amersham Biosciences). IPG strips were used according to the manufacturer's instructions. To obtain a detailed proteome map, four types of IPG strips were used: 18 cm immobilized pI 3-11 nonlinear, pI 3-5.6 nonlinear, pI 5.3-6.5 linear, and pI 6.2-7.5 linear. Samples containing 100-500 μg of soluble protein were diluted in 350 μL of rehydration solution (9 M urea, 2% CHAPS, 50 mM DTT, 2% IPG buffer) and applied to IPG strips by 12 hr rehydration at room temperature. Proteins were focused successively for 1 min at 500 V, 1 h 30 min at 3,500 V, 10 h at 3,500 V. After the first-dimensional IEF, IPG gel strips were placed in an equilibration buffer (6 M urea, 2% SDS, 30% glycerol, 50 mM Tris-HCl, pH 8.8) containing 1 M DTT for 15 min under agitation. The gels were then transferred to the equilibration solution containing 2.5% iodoacetamide and shaken for 15 min before they were placed on a 12.5% polyacrylamide gel slab. Separation in the second dimension was carried out in Tris-glycine buffer (25 mM Tris, 192 mM glycine) containing 0.1% SDS at a current setting of 40 mA for 4 hr. Following 2-DE, the gels were visualized with silver staining and were scanned at an optical resolution of 41.6 μm/pixel (EPSON expression 10000XL). Spot detection, quantification and matching were performed using Progenesis Samespots software version 3.0 (NonLinear).

In-gel Digestion

For MS fingerprinting and MS/MS analysis, the gel slices containing silver-stained protein spots were excised and transferred to a siliconized 1.5 mL Eppendorf tube (Sigma). Destaining solution (30 mM potassium ferricyanide/100 mM sodium thiosulfate (1 : 1)) was added to the tube to cover the gel piece, and the samples were vortexed until completely destained. The gel pieces were repeatedly washed, dehydrated in acetonitrile and dried in a vacuum centrifuge. The gel pieces were swollen in 20 μL of 50 mM ammonium bicarbonate buffer containing 5-10 ng/μL trypsin and were incubated overnight at 37˚C. The digest buffer was removed and the gel pieces were then extracted with 5% trifluoroacetic acid (TFA)/50% acetonitrile (ACN) solution. This extraction step was repeated three additional times.

MALDI-TOF Mass Spectrometry and Protein Identification

The matrix solution was prepared by dissolving 10 mg cyano-4-hydroxycinnamic acid (Sigma) in 1 mL of 50% acetonitrile and 0.1% trifluoroacetic acid in deionized water. The peptide digest (1 μL) was mixed with 1 μL of matrix solution and this mixture was applied to a stainless steel plate. Mass spectra were obtained using Applied Biosystems 4700 Proteomics Analyzer MALDI-TOF mass spectrometer equipped with Nd:YAG laser with a pulse width of 3 ns. The accelerating voltage was 25 kV, and the grid voltage was set at 70% of the accelerating voltage. After a delay of 350 ns, the accelerating voltage was used to extract the ions. After the acquisition of full scan mass spectra, MS/MS scans were acquired for the ten most intense ions using dynamic exclusion. A protein database search was performed with the Mascot search engine (Matrix Science, London, UK) using monoisotopic peaks against the NCBI nonredundant protein database. For proteolytic cleavages, only tryptic cleavage was allowed, and the number of maximal internal (missed) cleavage sites was set to 1. Variable modifications at cysteine with carboxyamidomethylation and methionine with oxidation were allowed. The mass tolerances of the precursor peptide ion and fragment ion were set to 100 ppm. Mascot scores greater than 65 for MS fingerprinting and Mascot scores greater than 35 for MS/MS spectra analysis were considered significant ($p < 0.05$).

Acknowledgements

This work was supported by intramural research funds of CbsBioscience, Inc (CBS-08-71).

References

1. Bosch, F.X., Ribes, J., Diaz, M. & Cleries, R. Primary liver cancer: Worldwide incidence and trends. *Gastroenterology* **127**, S5-16 (2004).
2. Stuver, S.O. Towards global control of liver cancer? *Semin. Cancer Biol.* **8**, 299-306 (1998).
3. Gupta, S., Bent, S. & Kohlwes, J. Test characteristics of alpha-fetoprotein for detecting hepatocellular carcinoma in patients with hepatitis C. A systematic review and critical analysis. *Ann. Intern. Med.* **139**, 46-50 (2003).
4. Seow, T.K., Liang, R.C.M.Y., Leow, C.K. & Chung, M.C.M. Hepatocellular carcinoma: from bedside to proteomics. *Proteomics* **1**, 1249-1263 (2001).
5. Yeom, Y.I., Kim, S.-Y., Lee, H.G. & Song, E.Y. Cancer biomarkers in 'Omics age. *BioChip J.* **2**, 160-174 (2008).
6. Cravatt, B.F., Simon, G.M. & Yates III, J.R. The biological impact of mass-spectrometry-based proteomics. *Nature* **450**, 991-1000 (2007).
7. Park, K.-S., Cho, S.Y., Kim, H. & Paik, Y.-K. Proteomic alterations of the variants of human aldehyde dehydrogenase isozymes correlate with hepatocellular carcinoma. *Int. J. Cancer* **97**, 261-265 (2002).
8. Park, K.-S. *et al.* Proteomic analysis and molecular

characterization of tissue ferritin light chain in hepatocellular carcinoma. *Hepatology* **35**, 1459-1466 (2002).
9. Cho, S.Y. *et al.* An integrated proteome database for two-dimensional electrophoresis data analysis and laboratory information management system. *Proteomics* **2**, 1104-1113 (2002).
10. Lim, S.O. *et al.* Proteome analysis of hepatocellular carcinoma. *Biochem. Biophys. Res. Commun.* **291**, 1031-1037 (2002).
11. Kim, J. *et al.* Proteome analysis of human liver tumor tissue by two-dimensional gel electrophoresis and matrixassisted laser desorption/ionization-mass spectrometry for identification of disease-related proteins. *Electrophoresis* **23**, 4142-4156 (2002).
12. Li, C. *et al.* Proteomic analysis of hepatitis B virus-associated hepatocellular carcinoma: Identification of potential tumor markers. *Proteomics* **5**, 1125-1139 (2005).
13. Luk, J.M. *et al.* Proteomic profiling of hepatocellular carcinoma in Chinese cohort reveals heat-shock proteins (Hsp27, Hsp70, GRP78) up-regulation and their associated prognostic values. *Proteomics* **6**, 1049-1057 (2006).
14. Lee, I.-N. *et al.* Identification of human hepatocellular carcinoma-related biomarkers by two-dimensional difference gel electrophoresis and mass spectrometry. *J. Proteome Res.* **4**, 2062-2069 (2005).
15. Melle, C. *et al.* Proteomic profiling in microdissected hepatocellular carcinoma tissue using ProteinChip technology. *Int. J. Oncol.* **24**, 885-891 (2004).
16. Sun, W. *et al.* Proteome analysis of hepatocellular carcinoma by two-dimensional difference gel electrophoresis: novel protein markers in hepatocellular carcinoma tissues. *Mol. Cell. Proteomics* **6**, 1798-1808 (2007).
17. Teramoto, R. *et al.* Protein expression profile characteristic to hepatocellular carcinoma revealed by 2D-DIGE with supervised learning. *Biochim. Biophys. Acta* **1784**, 764-772 (2008).
18. Blanc, J.-F. *et al.* Proteomic analysis of differentially expressed proteins in hepatocellular carcinoma developed in patients with chronic viral hepatitis C. *Proteomics* **5**, 3778-3789 (2005).
19. Yokoyama, Y. *et al.* Proteomic profiling of proteins decreased in hepatocellular carcinoma from patients infected with hepatitis C virus. *Proteomics* **4**, 2111-2116 (2004).
20. Garber, K. Energy boost: the Warburg effect returns in a new theory of cancer. *J. Natl. Cancer Inst.* **96**, 1805-1806 (2004).
21. Gatenby, R.A. & Gillies, R.J. Why do cancers have high aerobic glycolysis? *Nat. Rev. Cancer* **4**, 891-899 (2004).
22. Fulda, S., Wick, W., Weller, M. & Debatin, K.-M. Smac agonists sensitize for Apo2L/TRAIL- or anticancer drug-induced apoptosis and induce regression of malignant glioma in vivo. *Nat. Med.* **8**, 808-815 (2002).
23. Mizutani, Y. *et al.* Downregulation of Smac/DIABLO expression in renal cell carcinoma and its prognostic significance. *J. Clin. Oncol.* **23**, 410-412 (2005).
24. Seow, T.K. *et al.* Two-dimensional electrophoresis map of the human hepatocellular carcinoma cell line, HCC-M, and identification of the separated proteins by mass spectrometry. *Electrophoresis* **21**, 1787-1813 (2000).
25. Ou, K. *et al.* Proteome analysis of a human heptocellular carcinoma cell line, HCC-M: an update. *Electrophoresis* **22**, 2804-2811 (2001).
26. Cui, J.-F. *et al.* Differential proteomic analysis of human hepatocellular carcinoma cell line metastasis-associated proteins. *J. Cancer Res. Clin. Oncol.* **130**, 615-622 (2004).
27. Yang, Z.F. *et al.* Identification of brain-derived neurotrophic factor as a novel functional protein in hepatocellular carcinoma. *Cancer Res.* **65**, 219-225 (2005).
28. Cui, F. *et al.* The up-regulation of proteasome subunits and lysosomal proteases in hepatocellular carcinomas of the HBx gene knockin transgenic mice. *Proteomics* **6**, 498-504 (2006).
29. Schwegler, E.E. *et al.* SELDI-TOF MS profiling of serum for detection of the progression of chronic hepatitis C to hepatocellular carcinoma. *Hepatology* **41**, 634-642 (2005).
30. Poon, T.C.W. *et al.* Comprehensive proteomic profiling identifies serum proteomic signatures for detection of hepatocellular carcinoma and its subtypes. *Clin. Chem.* **49**, 752-760 (2003).
31. Paradis, V. *et al.* Identification of a new marker of hepatocellular carcinoma by serum protein profiling of patients with chronic liver diseases. *Hepatology* **41**, 40-47 (2005).
32. Comunale, M.A. *et al.* Comparative proteomic analysis of de-N-glycosylated serum from hepatitis B carriers reveals polypeptides that correlate with disease status. *Proteomics* **4**, 826-838 (2004).
33. Thorgeirsson, S.S. & Grisham, J.W. Molecular pathogenesis of human hepatocellular carcinoma. *Nat. Genet.* **31**, 339-346 (2002).
34. Lee, J.-S. & Thorgeirsson, S.S. Genome-scale profiling of gene expression in hepatocellular carcinoma: Classification, survival prediction, and identification of therapeutic targets. *Gastroenterology* **127**, S51-S55 (2004).
35. Kim, Y., Sills, R.C. & Houle, C.D. Overview of the molecular biology of hepatocellular neoplasms and hepatoblastomas of the mouse liver. *Toxicol. Pathol.* **33**, 175-180 (2005).
36. Roberts, L. & Gores, G. Hepatocellular carcinoma: molecular pathways and new therapeutic targets. *Semin. Liver Dis.* **25**, 212-225 (2005).
37. Rini, J., Szumlanski, C., Guerciolini, R. & Weinshilboum, R. Human liver nicotinamide N-methyltransferase: ion-pairing radiochemical assay, biochemical properties and individual variation. *Clin. Chim. Acta* **186**, 359-374 (1990).

38. Aksoy, S., Szumlanski, C. & Weinshilboum, R. Human liver nicotinamide N-methyltransferase. cDNA cloning, expression, and biochemical characterization. *J. Biol. Chem.* **269**, 14835-14840 (1994).
39. Kim, J. *et al.* Expression of nicotinamide N-methyltransferase in hepatocellular carcinoma is associated with poor prognosis. *J. Exp. Clin. Cancer Res.* **28**, 20 (2009).
40. Kim, J. *et al.* Real-time reverse transcription PCR analysis for validation of transketolase gene in hepatocellular carcinoma tissues. *BioChip J.* **3**, 130-138 (2009).
41. Edmondson, H. & Steiner, P. Primary carcinoma of the liver: a study of 100 cases among 48,900 necropsies. *Cancer* **7**, 462-503 (1954).